HERA MEMO: CLOSURE DIAGNOSTICS

JAMES KENT, CHRIS CARILLI, BOJAN NIKOLIC, NITHYANANDAN THYAGARAJAN,
AND ADAM BEARDSLEY

1. INTRODUCTION

One of the main design goals of HERA is to make a detection of the neutral hydrogen spin line. A great challenge to this is the extremely weak signal to noise ratio, necessitating a steady hand in calibration and dealing with radio foregrounds. The usage of closure phases in highly redundant arrays has been shown in Carilli et al. (2018), and has been posited as a way of directly measuring the 21cm hydrogen line, due to its ability to remove direction-independent effects (Thyagarajan et al., 2018).

This memo looks at using the closure phases for diagnostics on highly redundant arrays. It shows how the redundancy between identical closure triads in the array is poor, and indicates triads cannot be averaged together to reduce noise for the bispectrum method. It also points to an unevenness in the response of the telescope which serves to frustrate baseline power spectrum techniques.

Firstly we re-state the basic mathematical theory behind closure phases as well as discuss defining statistical measures on an angular dataset (the closure phase), and how it can be used as a direct measure of triad redundancy. From there we look at some metrics designed using the closures to explore the feasibility of averaging triads for detecting the neutral hydrogen line. More importantly it gives us great insight into the overall health of the telescope.

2. THEORY

The bispectrum is the calculated closure phase between three antennas over the frequency range of the telescope. Start first with the canonical visibility relation as per van-Cittert Zernike theorem (Born and Wolf, 1999):

$$V_{ab}(f) = \int F_a(\sigma, f) F_b^*(\sigma, f) I(\sigma, f) \exp[-i2\pi d_{ab} \cdot \sigma] d\Omega \tag{1}$$

Where, σ is the unit normal vector to a solid angle element, $d\Omega$, on the sky, f denotes the frequency of the measurement, d_{ab} denotes the vector joining the antenna pair a and b, $F_a(\sigma, f)$ and $F_b(\sigma, f)$ are the directional power patterns of the antennas a and b, and $I(\sigma, f)$ is the intensity distribution on the sky.

From this the closure phase or 'bi-spectrum' can be calculated as so:

$$C_{abc}(f) = V_{ab}(f)V_{bc}(f)V_{ca}(f) \tag{2}$$

In the presence of a strong point source, the antenna responses cancel and the closure phase should be zero. As directional-dependent and baseline-dependent effects become prominent, the instrumental phases no longer cancel. This means the closure phases are not free of instrumental corruption anymore.

Start with assumption that measured closure phase measured on same triangle at same LST on different days differs only by circular Gaussian random noise as per the Wrapped Normal Distribution (Mardia and Jupp, 2008), i.e.:

$$\phi_{i,j,k}(\nu,t;D) = \hat{\phi}_{i,j,k}(\nu,t) + \varepsilon \tag{3}$$

where $\phi_{i,j,k}(\nu,t;D)$ is closure phase measured on triangle i,j,k at frequency ν and local sidereal time t and date D, $\hat{\phi}_{i,j,k}(\nu,t)$ is the underlying true closure phase and $\varepsilon \sim WN(0,\sigma_\nabla)$ where σ_∇ is the noise on a triangle. We can estimate the noise σ_∇ by calculating the standard deviation of $\phi_{i,j,k}(\nu,t;D)$ across different days assuming the closure phase across different days differs only by noise.

The standard deviation σ_∇ is calculated as Mardia and Jupp (2008) by first wrapping the phases around the unit circle: $cos(\phi_i) + isin(\phi_i) = e^{i\phi}$. The mean resultant vector inside the unit disk is calculated:

$$\frac{1}{N}\sum_{x=0}^{N} cos(\phi_x) + \frac{i}{N}\sum_{x=0}^{N} sin(\phi_x) = \bar{R}e^{i\bar{\phi}} \tag{4}$$

where ϕ_x represents each closure measurement at a particular $\phi_{i,j,k}(\nu,t;D)$, thus N measurements, such that $x = 1,2,..,N$. The set of measurements of size N is that of all triads of same size and orientation. As $0 < \bar{R} < 1$ we can use it as a measure of how concentrated the closure measurements at a particular channel at a particular timestamp are. If they are highly concentrated($R \sim 1$) then the closures are measuring almost the same thing and redundancy is good. If $R << 1$ then redundancy is poor. It is a direct measure of redundancy. Using the characteristic function of the wrapped gaussian is:

$$\int_0^{2\pi} e^{in\theta} f_{WN}(\phi;\bar{\phi},\sigma)d\phi = e^{in\bar{\phi}-\frac{n^2\sigma^2}{2}} \tag{5}$$

Where f_{WN} is the characteristic function of the wrapped normal distribution. Thus we arrive at the above considering integer values of n:

$$e^{i\bar{\phi}-\frac{\sigma^2}{2}} = \bar{R}e^{i\bar{\phi}} \tag{6}$$

From $\bar{R} = e^{-\frac{\sigma^2}{2}}$ we can then calculate standard deviation on the circle as $\sigma_\nabla = \sqrt{-2\ln(\bar{R})}$. The mean closure phase is calculated as:

$$\bar{\phi}_{\nabla\mathrm{EQ14}}(v,t;D) = \tan^{-1}\left(\frac{\bar{S}}{\bar{C}}\right) \tag{7}$$

Where $\bar{S}$ and $\bar{C}$ are the sine and cosine terms of $\bar{R}e^{i\bar{\phi}}$. $\bar{\phi}_{\nabla\mathrm{EQ14}}$ represents the mean closure phase of the set of equilateral triangles with 14m baselines at a particular frequency and LST. From this we can find the average of all triads on a single LST, and then average those averages over successive LST's to reduce the noise. The set of averages, with each element of the set denoting the averaged triads on a single LST, can be used for finding the standard deviation as above.

3. Redundancy Between Triangles

Using the circular statistics established above, an overall measure of telescope performance can be created. Some broad results are presented alongside some finer grained breakdown of the redundancy between telescopes.

The primary triad configuration of interest is 14m equilateral north/south facing triads. We first consider the standard deviation across the telescope as a function of both Local Sidereal Time (LST) and Frequency Channel. The deviation between 14m equilateral triads is shown for Julian Dates 2458102 and 2458124 in Figures 1 and 3, respectively.

You will notice the strongly frequency dependent nature of the divergences between triads over time. The general shape of the 'disturbances' in triad redundancy is very consistent across days. This could be indicative of a direction dependent effect which is indicative of some issue in the beam shapes of the telescope or repeating complicated sky

0.16	0.0852
0.0852	0.17

TABLE 1. Covariances of noise and standard deviations.

structure coupled with beam shape, over something such as the electronics. This consistency across days was tested up to a month into the future and there was no change at all in the distribution apart from a slow drift, which is a result of the difference in time between the solar day and the sidereal day.

The sun was first though to be the cause of the serious disturbances on the left hand side of these plots, around LST x.1019. But looking a month later it is noticed that the shape of the plots doesn't change much at all even when the sun is up. The question this plot raises is clear: why do have these breakdowns in redundancy that replicate at the same sidereal time every single day? Work by Adam Beardsley and co. at ASU has pointed out the island of convergence at LST x.13 is due to Fornax being in the beam, pushing all of the closures close to zero.

There is a small correlation between the Noise to Signal Ratio and standard deviation measured as:

$$NSR = \frac{\left[V_{00}V_{11}V_{22}\right]^{\frac{1}{3}}}{\left[V_{01}V_{12}V_{20}\right]^{\frac{1}{3}}} \tag{8}$$

This is shown in Figure 5, and the covariances are shown in Table 1 after the NSR is normalised to have an identical mean to the standard deviation. This covariance matrix was diagonalised, and the eigenvalues found, and the correlated and uncorrelated terms plotted in Figure 6. There is a strong correlation however it doesn't explain systematic divergences noticed in fields with a lower NSR, such as the Fornax A field.

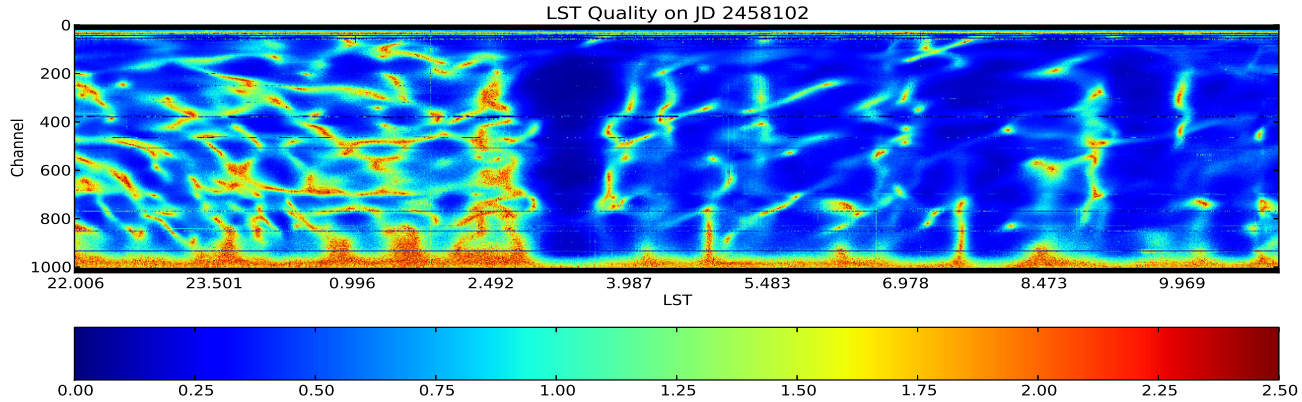

FIGURE 1. Standard deviation (Radians) between 45 14 m equilateral triads as a function of LST and Frequency at JD 2458102 on XX polarisations. The divergence in closures between triads is frequency dependent with all channels rarely behaving at the same time. Around LST 3h, there is a convergence, which is mainly caused by the transit of Fornax.

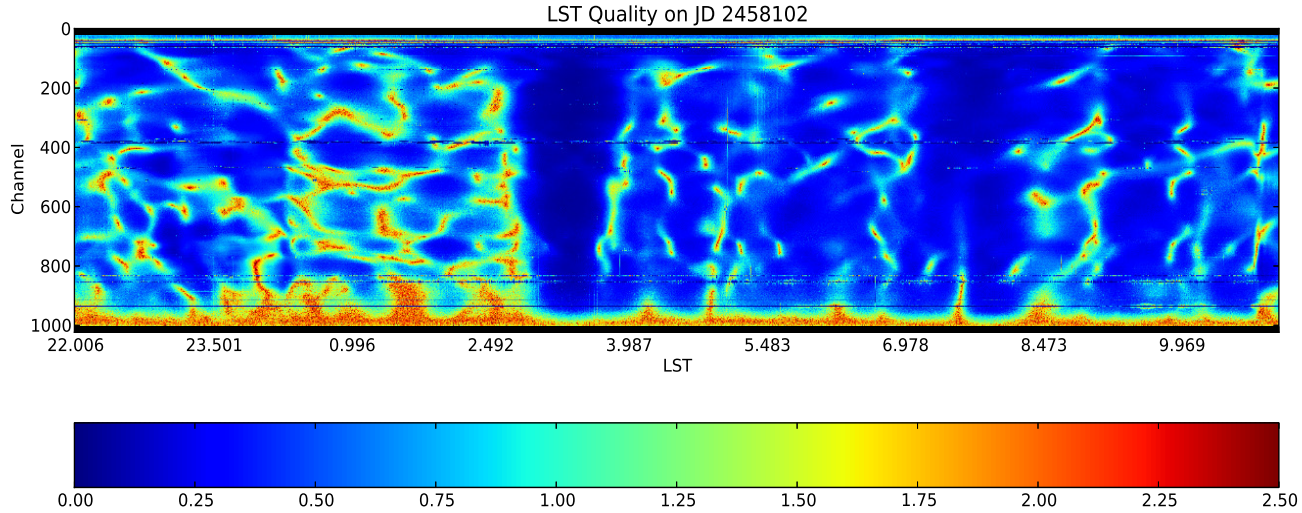

FIGURE 2. Standard deviation between 45 14 m equilateral triads as a function of LST and Frequency at JD 2458102 on YY polarisations. Fornax transiting still causes convergence around LST 3h.

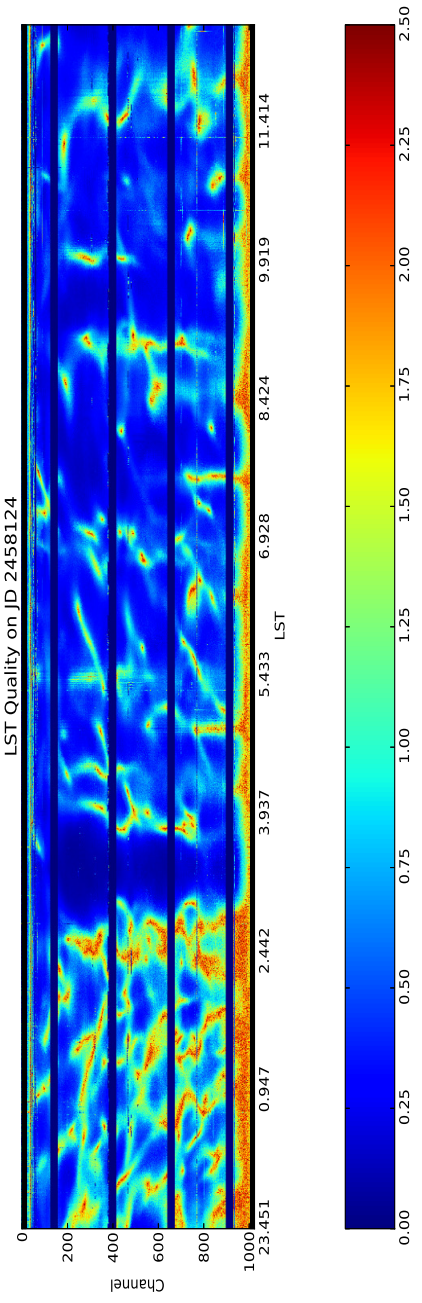

FIGURE 3. Standard deviation between 45 14 m equilateral triads as a function of LST and Frequency at JD 2458124. There is a lot of channel corruption on this date but we can see the overall shape of closure divergences is unchanged. The only difference between this and JD 2458102 is the sky drifting by roughly four minutes each night.

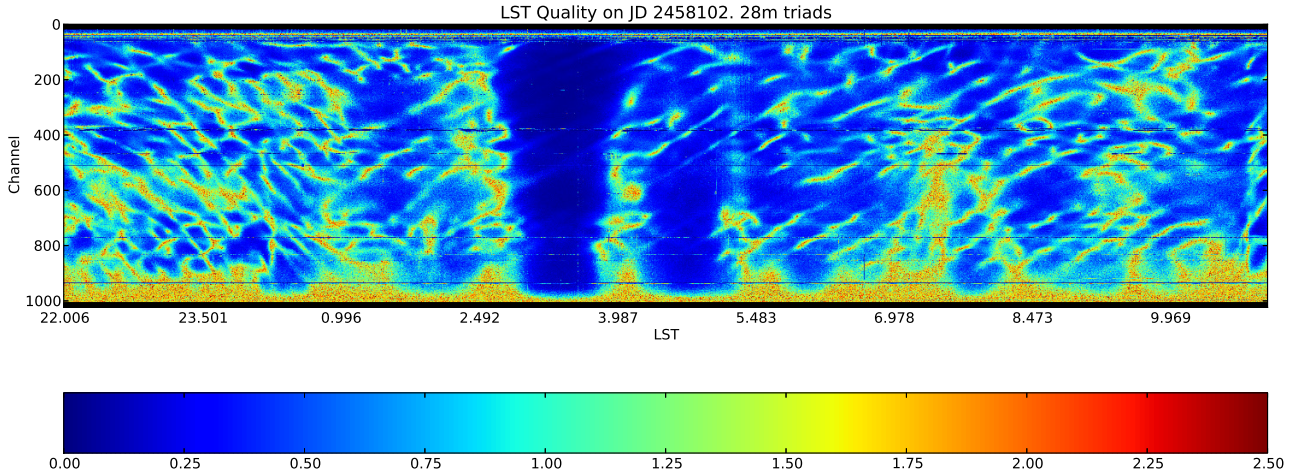

FIGURE 4. Standard deviation between 12 28 m equilateral triads as a function of LST and Frequency on JD 2458102. The divergence in closures between triads is frequency dependent with all channels rarely behaving at the same time. After the sun sets, there is an hour of excellent convergence, why this is the case is not known.

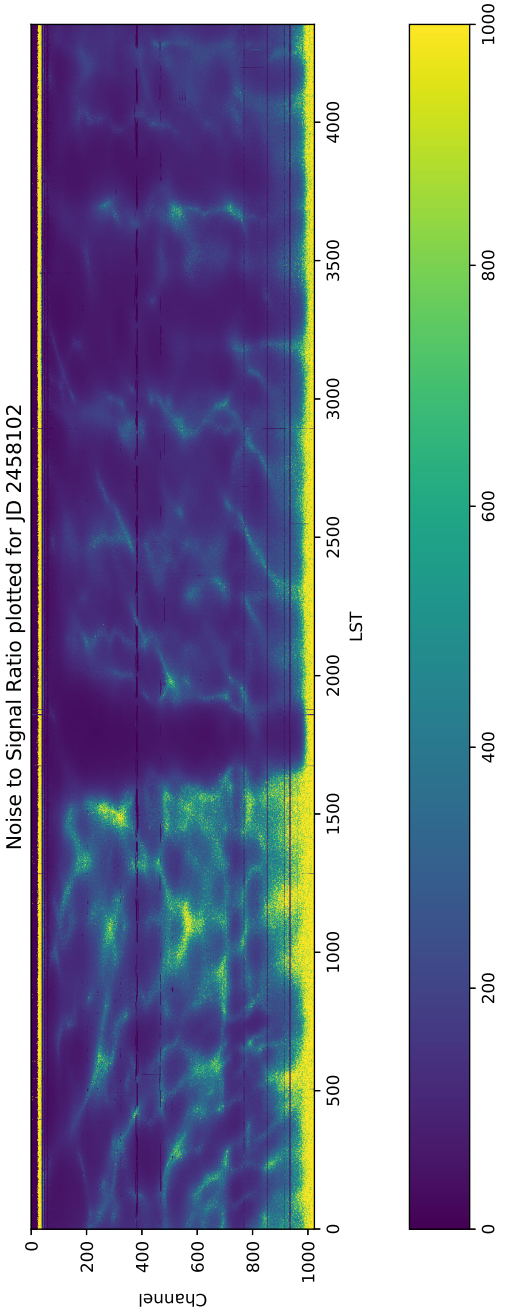

FIGURE 5. Noise to Signal Ratio plotted as the third root of the product of the autocorrelations divided by the third root of product of the cross-correlations for an EQ14 triads.

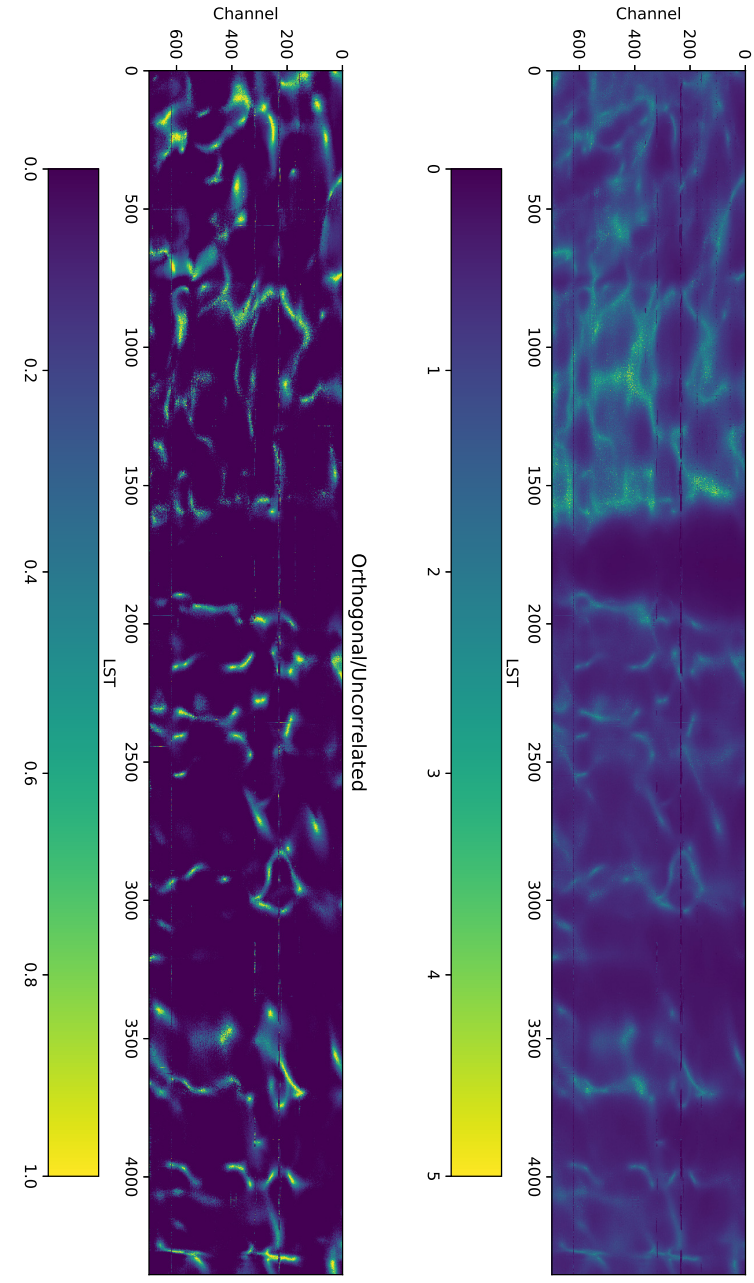

FIGURE 6. Linear combination weighted by eigenvalues of the standard deviation and Noise-Signal Ratio measured on JD 2458102.

3.1. **Effect of Individual Antennas.** In addition to judging the overall triad performance, it's important to see wether there are particularly wayward antennas dragging performance down. We do this by borrowing a technique from the sport of rowing. Prospective athletes are raced in a boat and their performance timed, they are then swapped out for another rower. If the boat then goes faster, they lose their seat race, and vice versa. We apply the same logic to triads in our set of measurements: if we remove a triad and standard deviation decreases, it's likely the triad includes an antenna with a response very dissimilar from another.

To do this, we choose two LST's, one with particularly good redundancy, and one with much lower redundancy between triads. These are shown in Figures 7 and 8. For the well behaved LST it can be seen that removing most triads causes a small increase in the gaussian noise, alongside what we would expect from theory. However we can still see there are errant antennas where standard deviation actually decreases when they are removed, indicating they are an outlier causing. From this we can see that antennas 38 and 53 have odd closure characteristics, and 24 and 25 are also suspect.

The bad LST in Figure 8 shows that this method breaks down when the redundancy is very poor, due to all the triads measuring their own true closure phase, thus following seperate distributions. In this case, all antennas are misbehaving relative to the others, for a reason that is currently unknown.

3.2. **Pairwise Triad Distance.** Another method to compare antennas is to do a brute force exploration of some distance space defined by a pairwise combination of each triad with every other triad. This constructs a hollow matrix as so:

$$\xi = \begin{bmatrix} 0 & \delta_{1,2} & \dots & \delta_{1.N} \\ \delta_{2,1} & 0 & \dots & \delta_{2,N} \\ \vdots & \vdots & \ddots & \vdots \\ \delta_{N,1} & \delta_{N,2} & \dots & 0 \end{bmatrix} \tag{9}$$

Where $\delta_{i,j}$ is the mean euclidean distance between the closure measurements in all channels.

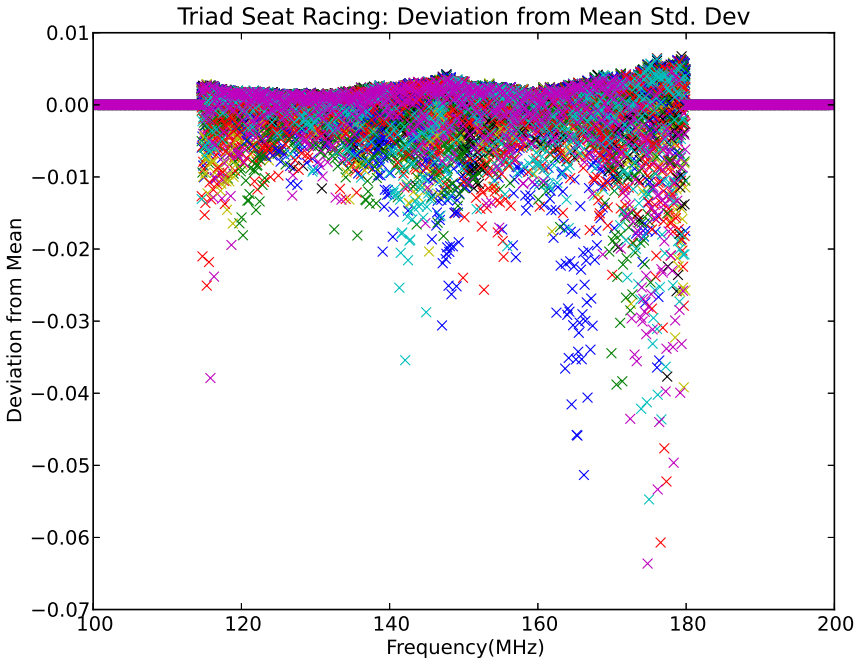

FIGURE 7. Deviations from the mean standard deviations at LST 64829.1352464 at 2458098.34922. For each triad when it is removed from the overall set of triads. There are significant frequency dependencies in how each triad is affected.

$$\delta_{i,j} = \frac{1}{M}\sum_{x=0}^{M}\left[(\cos C_{i,x} - \cos C_{j,x})^2 + (\sin C_{i,x} - \sin C_{j,x})^2\right]^{\frac{1}{2}} \tag{10}$$

Where x is the frequency channels. A direct plot of the matrix defined in (9) for our good LST taken on 2458098.34922, is shown in Figure 9.

Then each row of the matrix in (9) is sorted in ascending order, to find pairs of triads with the lowest mean distance between them. Patches of antennas with similar closure measurements begin to appear. It is noticed that in the good LST(x.1352464) and bad LST triads 22, 23, 24, 25 have relatively low distance measurements compared to each other. There are still noticeable systematic divergences between them. These are shown in Figure 10. Despite the closures being on top of each other (within noise) for most of the spectrum, there are broad chunks of spectrum where they diverge even if a small amount. This small

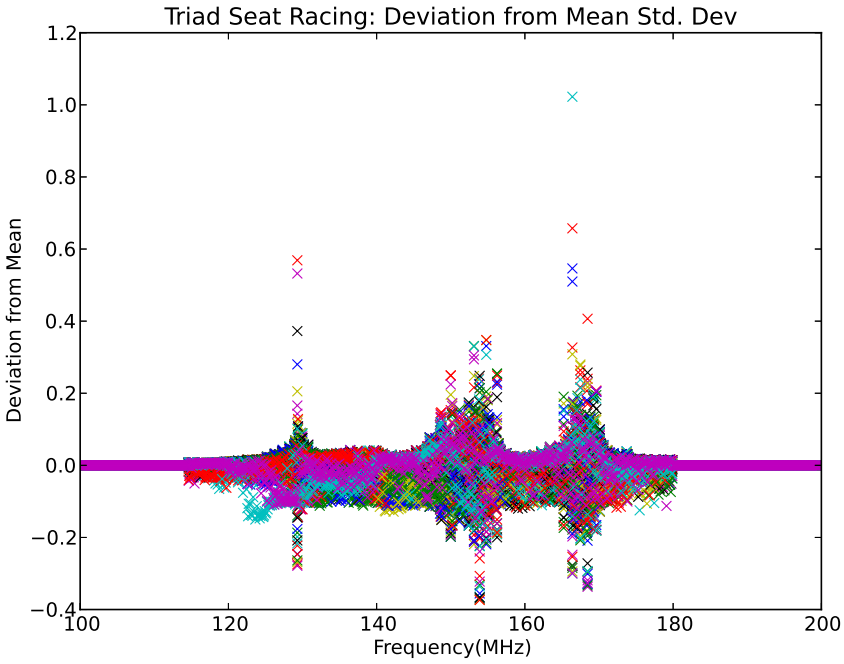

FIGURE 8. Deviations from the mean standard deviations at LST 64829.37538083 at 2458098.58782. The difference between this and Figure 7 is significant, and shows the general lack of redundancy.

amount is (likely?) much larger than expected EoR oscillations. The divergences are of a frequency dependent nature, and it is currently unclear why this is happening.

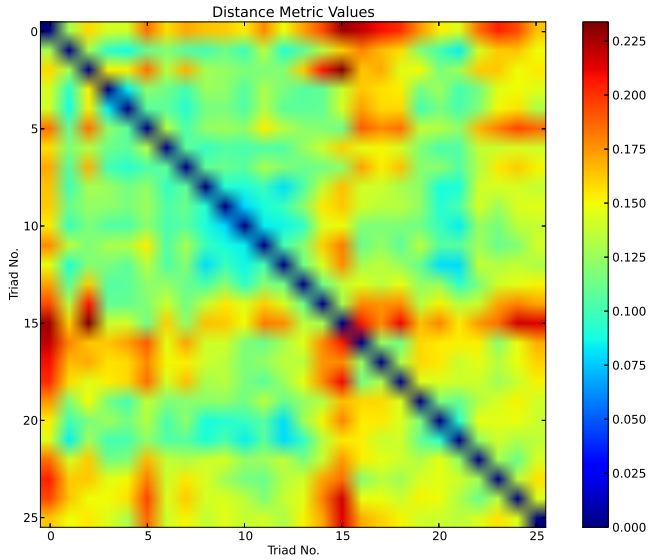

FIGURE 9. Direct plot of Pairwise Distance Matrix. The closer to zero the more similar the triads. From this we can directly find outlier triads and triangulate particularly bad antennas. We can also notice patches of redundancy in the telescope.

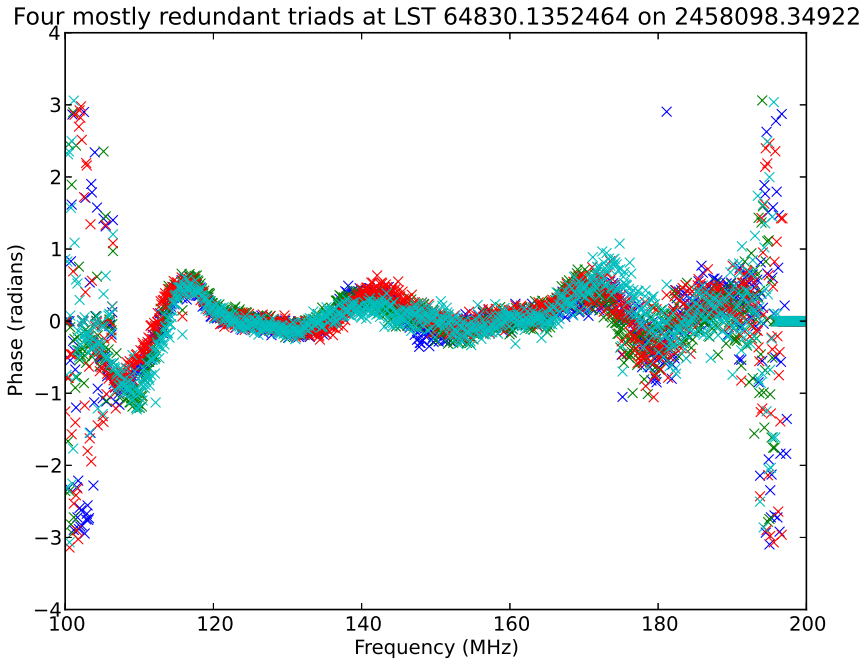

FIGURE 10. Four (mostly) redundant triads at LST 64829.1352464, during Fornax's transit. The triads are [120, 121, 140] (Dark Blue), [121, 122, 141] (Green), [122,123,142] (Red), [123,124,143] (Light Blue). Notice that despite the excellent concentration and standard deviation at this LST there is still a systematic effect in play especially in the frequencies between 138-148MHz.

4. DISCUSSION

From theory it is known that geometrically like-for-like triads should measure the exact closure phase, within noise. A strong noise to signal ratio causes the overall scatter of the closures, η in our notation, to increase. However the closure bias from some true closure also increases, as seen by the systematic deviation in closures such as in Figure 10, which is what our statistics in Figures 1, 2, 3 and 3 show.

This approach does reveal a lot about the overall health of the telescope, in terms of redundancy and similarity between antennas. Using the statistics defined by the wrapped Gaussian, we can measure the overall redundancy between triads and across the telescope. This has been done here and shows that redundancy is not ideal, and points to a direction-dependent effect in the telescope due to the closures negation of direction-independent effects. This is very difficult to calibrate out due to no exact beam models existing for every antenna.

Using triad seat racing, as well as brute force exploration of the distance space between all triads, allows us to see which triads are performing poorly compared to others in the array, and allow us to triangulate antennas of dubious performance.

There is a subtle effect of some patches of antennas being more redundant with each other, potentially due to electronics or coupling effects. However this effect is not dominant, and should not distract from the overall lack of redundancy across the telescope.

5. CONCLUSION

From what we have seen it can be shown that redundancy between identical triads, and resultingly, antennas is inconsistent. What the closure phases are showing us is that there is a significant issue across the whole telescope which causes the closure phases to diverge. The consistent closure standard deviation response at the same LST indicates this is an issue with the beam shapes of the telescope and source structure which do not change. With more complicated Sky Brightness Distributions and higher NSR's we see an overall amplification of the effect caused by some underlying redundancy.

The closures here can form another chain in the quality assurance pipeline. The nature of the bi-spectrum as a calibration independent observable yields interesting quality metrics for theoretically redundant arrays such as HERA, due to its ability to negate direction-independent calibration terms.

Future work will concentrate on understanding why this poor redundancy exists across the telescope, and trying to implement closure analysis as an extra step in the QA pipeline. Closure phases can be used to measure non-closing errors in the telescope which correspond to direction-dependent differences such as beam shapes. Additional follow-up work is required to work out exactly which antennas contribute to this.

REFERENCES

Born, M. and Wolf, E. (1999). *Principles of optics: electromagnetic theory of propagation, interference and diffraction of light*. Cambridge University Press, Cambridge, 7th (expanded) ed edition.

Carilli, C. L., Nikolic, B., Thyagarajan, N., Gale-Sides, K., Abdurashidova, Z., Aguirre, J. E., Alexander, P., Ali, Z. S., Balfour, Y., Beardsley, A. P., Bernardi, G., Bowman, J. D., Bradley, R. F., Burba, J., Cheng, C., DeBoer, D. R., Dexter, M., de˜Lera˜Acedo, E., Dillon, J. S., Ewall-Wice, A., Fadana, G., Fagnoni, N., Fritz, R., Furlanetto, S. R., Ghosh, A., Glendenning, B., Greig, B., Grobbelaar, J., Halday, Z., Hazelton, B. J., Hewitt, J. N., Hickish, J., Jacobs, D. C., Julius, A., Kariseb, M., Kohn, S. A., Kolopanis, M., Lekalake, T., Liu, A., Loots, A., MacMahon, D., Malan, L., Malgas, C., Maree, M., Martinot, Z., Matsetela, E., Mesinger, A., Molewa, M., Morales, M. F., Neben, A. R., Parsons, A. R., Patra, N., Pieterse, S., La Plante, P., Pober, J. C., Razavi-Ghods, N., Ringuette, J., Robnett, J., Rosie, K., Sell, R., Sims, P., Smith, C., Syce, A., Williams, P. K. ˜., and Zheng, H. (2018). HI 21cm Cosmology and the Bi-spectrum: Closure Diagnostics in Massively Redundant Interferometric Arrays. *arXiv:1805.00953 [astro-ph]*. arXiv: 1805.00953.

Mardia, K. V. and Jupp, P. (2008). Basic Concepts and Models. In *Directional Statistics*, pages 25–56. Wiley-Blackwell.

Thyagarajan, N., Carilli, C. L., and Nikolic, B. (2018). Detecting Cosmic Reionization Using the Bispectrum Phase. *Physical Review Letters*, 120(25).

E-mail address: jck42@cam.ac.uk

E-mail address: ccarilli@nrao.edu

E-mail address: bn204@cam.ac.uk

E-mail address: t_nithyanandan@nrao.edu

E-mail address: adam.p.beardsley@gmail.com